Chapter 3

Engineering Applications of Time-periodic Time-delayed Systems

Gábor Stépán

Department of Applied Mechanics
Budapest University of Technology and Economics
Muegyetem rkp 3*, Budapest H*-1111*, Hungary*
stepan@mm.bme.hu

Time delays often occur in engineering systems related to mechanical contact tasks and/or control tasks with relevant information processing and transmission time. Parametric excitation is also a typical vibration phenomenon in many well-known engineering applications. There are not many models, however, that combine delay and time-periodic coefficients, in spite of the fact that machine tool vibrations and many control problems, especially digital control tasks, may often lead to time-periodic delay differential equations with discrete delays or even with distributed ones. A paradigm for such delayed time-periodic systems is the delayed Mathieu equation, the stability analysis and stability charts of which will be presented. Then the numerical method called semi-discretization is introduced as a time-periodic perturbation of the time delay. Among the applications, the milling process and turning with spindle-speed variation is mentioned, while the so-called "act-and-wait" control is presented for robotic force control problems.

1. Introduction

Mathematical modeling of engineering systems with delay-differential equations has become increasingly efficient and popular as the mathematical theory developed during the recent decades. This process started with the proper formulation of the infinite dimensional state spaces of these systems by Myshkis[1], continued with the generalization of Floquet Theory to delay systems by Halanay[2], then followed by the construction of a unified theory for functional differential equations by Hale[3], then by Hale and Lunel[4] and many others.

However, engineering problems leading to delay-differential equation (DDE) models appeared much earlier, and they provided a driving force for the development of the mathematical theory. The famous population dynamics models of Volterra[5] in the 1920's already included time delays and produced oscillatory behavior observed in nature even for first order scalar systems. From mechanical engineering view-point, however, the second order models are relevant since many

of them are based to Newton's Laws where the acceleration appears as second derivative of the state variable. The corresponding models are also called *delayed oscillators*. These are oscillatory even without time delay, so the presence of delay makes their dynamics quite intricate.

The classical self-excited vibrations in the delayed oscillators are described by autonomous DDEs. Parametric excitation, however, is also an important source of oscillations, and the corresponding delayed oscillators are often governed by time-periodic non-autonomous DDEs. In the subsequent section of this review paper, the delayed Mathieu equation paradigm is discussed leading to the presentation of the corresponding stability chart. In Section 3, the basic idea of the semi-discretization method is summarized for the numerical stability analysis of large systems. Then two time-periodic DDE models are derived for milling processes: the first involves time-periodic coefficients; the second involves time-periodic time delays. Finally, the act-and-wait control concept is presented for a force-control problem with delay, which is an application of time-periodic gains for controlling delayed oscillators.

2. Delayed Mathieu Equation

The linear non-autonomous DDEs are considered in the general form

$$\dot{\mathbf{y}}(t) = \int_{-\tau_{\max}}^{0} \mathbf{y}(t+\vartheta) d_{\vartheta} \boldsymbol{\eta}(t,\vartheta) \,, \tag{1}$$

which is the representation of a linear non-autonomous functional differential equation $\dot{\mathbf{y}}(t) = L\,\mathbf{y}_t$ by means of a Stieltjes-integral in accordance with the Riesz Representation Theorem (see Hale[3]). Here $\mathbf{y}_t(\vartheta) = \mathbf{y}(t+\vartheta)$, $\vartheta \in [-\tau_{\max}, 0]$ is a function in the space $C^0_{[-\tau_{\max},0]}$ of continuous functions mapping the given time interval of length $\tau_{\max}$ into $\mathbb{R}^n$, and the $n \times n$ matrix $\boldsymbol{\eta}$ is a function of bounded variation in its second variable. If $\boldsymbol{\eta}$ is also time-periodic in its first variable, that is, $\boldsymbol{\eta}(t+T,\,\cdot\,) = \boldsymbol{\eta}(t,\,\cdot\,)$, then a time-periodic DDE is presented in (1).

It is well-known that all high order differential equations can be transformed into first order high dimensional differential equations. Since the Newtonian systems involve second time derivatives, the simplest delayed oscillator can be represented in the form of a 2-dimensional system. As the basic example for a delayed and parametrically excited oscillator, let us choose the measure $\boldsymbol{\eta}$ in the following simple form:

$$\boldsymbol{\eta}(t,\vartheta) = \begin{cases} \begin{bmatrix} 0 & 0 \\ 0 & 0 \end{bmatrix}, & \vartheta \in [-4\pi, -2\pi), \\ \begin{bmatrix} 0 & 0 \\ b & 0 \end{bmatrix}, & \vartheta \in [-2\pi, 0), \qquad t \in [t_0 - 2\pi, \infty), \\ \begin{bmatrix} 0 & 1 \\ b - (\delta + \varepsilon\cos t) & 0 \end{bmatrix}, & \vartheta = 0, \end{cases} \tag{2a}$$

and substitute it into (1) by using Stieltjes calculus $d_\vartheta \boldsymbol{\eta}(\,\cdot\,,\vartheta) = \dfrac{d}{d\vartheta}\boldsymbol{\eta}(\,\cdot\,,\vartheta)$ where $\boldsymbol{\eta}$ is differentiable, and $d_\vartheta \boldsymbol{\eta}(\,\cdot\,,\vartheta) = \boldsymbol{\eta}(\,\cdot\,,\vartheta) - \boldsymbol{\eta}(\,\cdot\,,\vartheta - 0)$ where it is discontinuous. The resulting periodic DDE will have the form

$$\begin{bmatrix} \dot{y}_1(t) \\ \dot{y}_2(t) \end{bmatrix} = \begin{bmatrix} 0 & 1 \\ -(\delta + \varepsilon \cos t) & 0 \end{bmatrix} \begin{bmatrix} y_1(t) \\ y_2(t) \end{bmatrix} + \begin{bmatrix} 0 & 0 \\ b & 0 \end{bmatrix} \begin{bmatrix} y_1(t-2\pi) \\ y_2(t-2\pi) \end{bmatrix} . \tag{2b}$$

After the introduction of the notation $x := y_1$, this can be transformed to the scalar second order periodic DDE

$$\ddot{x}(t) + (\delta + \varepsilon \cos t\,)x(t) = bx(t-2\pi)\,, \tag{3}$$

which is also called *delayed Mathieu equation*, since it gives the Mathieu[6] equation for $b = 0$, while it describes the delayed oscillator (see Bhatt and Hsu[7]) for $\varepsilon = 0$. This equation is special in the sense that the time-periodicity and the time delay are both equal to 2π. Still, this special case is important since a closed form analytical stability chart can be constructed, and also some mechanical models like those of milling operations have the same property, the delay and the time periodicity are just equal to each other.

The stability charts present those parameter domains where the trivial solution $x(t) \equiv 0$ is stable in Lyapunov sense. For the special case $b = 0$, the chart in the (δ, ε) parameter plane was constructed by van der Pol and Strutt[8] and can also be found in the book of Ince[9], while the chart in the (δ, b) parameter plane for $\varepsilon = 0$ is presented, for example, in the books of Stepan[10], Hu and Wang[11] or Michiels and Niculescu[12].

The stability chart in the 3-dimensional (δ, b, ε) parameter space can be determined by the application of the infinite dimensional extension of the Floquet theory and the analytical calculations can be carried out by means of the generalization of Hill's infinite dimensional determinant method. The details of this calculation together with its proof are presented in Insperger and Stepan[13] and the resulting stability chart is shown in Fig.1. Clearly, it is a kind of direct product of the two special cases discussed above, that is, the stability boundaries can be obtained by

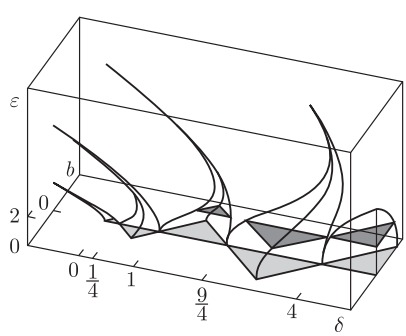

Fig. 1. Stability chart of the delayed Mathieu equation (3). Sections of stable regions are shaded.

shifting the tongues of the Strutt-Van der Pol stability chart along the triangles of the Bhatt-Hsu stability chart.

Along the stability surfaces, all the three kinds of possible bifurcations in periodic systems will appear: Neimark-Sacker (or secondary Hopf), flip (or period doubling), and fold (or secondary saddle-node) as explained by Insperger and Stepan[13].

3. Semi-discretization Method for Periodic DDEs

The stability of parametrically excited delayed oscillators can rarely be studied analytically. The delayed Mathieu equation paradigm discussed in the previous section is one of these exceptions that serves also as a test example for checking the numerical methods developed during the last decade, like the semi-discretization method of Insperger and Stepan[14], its version improved by Sheng, Elbeyly, and Sun[15], the time finite element method of Bayly, Halley, Mann, and Davies[16], the Chebishev polynomial method of Butcher et al.[17], the pseudo-spectral method of Breda, Maset, and Vermiglio[18]. In this section, the semi-discretization method is discussed as a numerical method based on the introduction of a special time-periodic time delay, that is, the introduction of a special parametric excitation for the delay itself.

Consider the delayed oscillator with constant parameters $c_{0,1}$ in the form of the scalar second order autonomous DDE

$$\ddot{x}(t) + c_0 x(t) = c_1\, x(t - 2\pi)\,, \tag{4}$$

and also an approximating delayed oscillator

$$\ddot{x}(t) + c_0 x(t) = c_1 x(t - \tau(t)) \tag{5}$$

with the time-periodic delay

$$\tau(t) = t + (m - \text{int}\ (t/\Delta t))\Delta t\,, \tag{6}$$

which is periodic with the time-step $\Delta t = 2\pi/(m+1/2)$ where m is an appropriately chosen integer, also called approximation number. As Fig.2 shows, the constant time delay 2π can be approximated as $m \to \infty$.

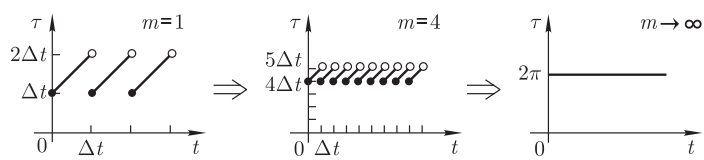

Fig. 2. Periodic time delays approximating constant time delay.

First, it may look unusual why an autonomous system is approximated by a non-autonomous one, but the special time periodicity of the delay results in a piecewise constant term in the right-hand-side of (4) for the intervals $t \in [t_i, t_{i+1}) =$

$[\, i\Delta t\,,\, (i+1)\Delta t\,)$, $i = 0, 1, 2, \ldots$ since

$$x(t-\tau(t)) \equiv x((i-m)\Delta t) =: x_{i-m}. \tag{7}$$

This way, an infinite series of non-homogeneous ordinary differential equations (ODE) has to be solved with concatenated initial conditions:

$$\ddot{x}(t) + c_0 x(t) = c_1 x_{i-m}, \quad x(t_i) = x_i,\ \dot{x}(t_i) = \dot{x}_i\,. \tag{8}$$

By means of the initial conditions, the coefficients K_{1i}, K_{2i} in the general solution

$$x(t) = K_{1i}\cos(\sqrt{c_0}t) + K_{2i}\sin(\sqrt{c_0}t) + \frac{c_1}{c_0}x_{i-m}, \quad t \in [t_i, t_{i+1}) \tag{9}$$

can be expressed by means of $x_i,\ \dot{x}_i,\ x_{i-m}$. Consequently, when $x_{i+1} := x(t_{i+1}) = x(t_i + \Delta t)$ is calculated in (9), then x_{i+1} can be expressed as a linear combination of $x_i,\ \dot{x}_i,\ x_{i-m}$. The same calculation can be repeated for $\dot{x}_{i+1}$. If all these values are collected in the vector $\mathbf{y}_i = \mathrm{col}\ (\dot{x}_i\ x_i\ x_{i-1}\ \cdots\ x_{i-m}) \in \mathbb{R}^{m+2}$, then a linear map is compiled and the so-called characteristic multipliers are calculated

$$\mathbf{y}_{i+1} = \mathbf{A}\mathbf{y}_i \quad \Rightarrow \quad \det(\mu\,\mathbf{I} - \mathbf{A}) = 0 \quad \Rightarrow \quad \mu_{1,2,\ldots,m+2}. \tag{10}$$

The coefficient matrix $\mathbf{A}$ is a constant and all its elements are expressed by the coefficients $c_{0,1}$ of the original delayed oscillator (4) and the approximation parameter m. The stable parameter regions in the parameter plane are determined by the condition $|\mu_{1,2,\ldots,m+2}| < 1$. The larger m is, the better the stability chart is approximated, as it is shown in Fig.3. For $m = 10$, the exact triangle-shaped stability chart (see the shaded regions for $\varepsilon = 0$ in Fig.1.) is already well approached.

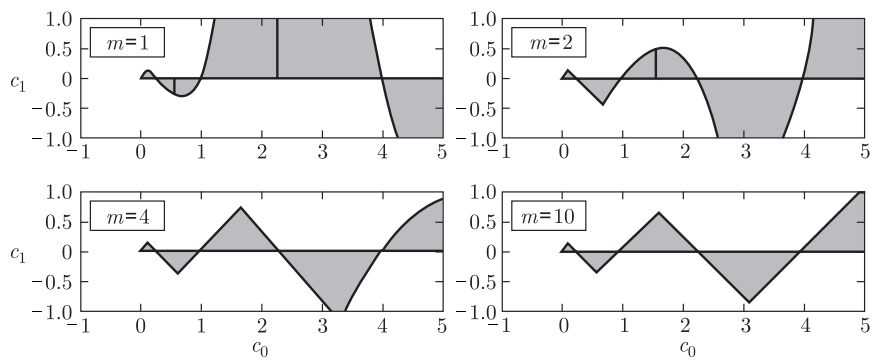

Fig. 3. Approximate stability charts of the delayed oscillator (4). Stable regions are shaded.

A piece-wise constant approximation for the Mathieu equation

$$\ddot{x}(t) + (\delta + \varepsilon\cos t)x(t) = 0 \tag{11}$$

is already a well-known method in the form

$$\ddot{x}(t) + c_{0i}x(t) = 0, \quad x(t_i) = x_i,\ \ \dot{x}(t_i) = \dot{x}_i \tag{12}$$

for $t \in [t_i, t_{i+1}) = [\, i\Delta t\,,\, (i+1)\Delta t\,)$, $\Delta t = 2\pi/m$ with $c_{0i} = \delta + \varepsilon \cos t_i$ (see also Fig.4).

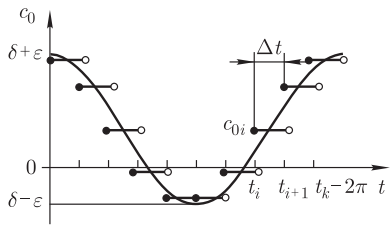

Fig. 4. Approximation of harmonic parameter excitation in the Mathieu equation.

The piece-wise specific solution of (12) is

$$x(t) = x_i \cos\left(\sqrt{c_{0i}}(t-t_i)\right) + \frac{\dot{x}_i}{\sqrt{c_{0i}}} \sin\left(\sqrt{c_{0i}}(t-t_i)\right)\ , \quad t \in [t_i, t_{i+1})\,, \tag{13}$$

which means that again, the calculation of $x_{i+1} := x(t_{i+1}) = x(t_i + \Delta t)$ leads to the construction of a discrete map for the vector $\mathbf{y}_i = \mathrm{col}(x_i\ \dot{x}_i) \in \mathbb{R}^2$ in the form

$$\mathbf{y}_{i+1} = \mathbf{A}\mathbf{y}_i, \quad \mathbf{A}_i = \begin{pmatrix} \cos\left(\Delta t\sqrt{c_{0i}}\right) & \dfrac{\sin\left(\Delta t\sqrt{c_{0i}}\right)}{\sqrt{c_{0i}}} \\ -\sqrt{c_{0i}}\sin\left(\Delta t\sqrt{c_{0i}}\right) & \cos\left(\Delta t\sqrt{c_{0i}}\right) \end{pmatrix}. \tag{14}$$

Then the subsequent application of this iteration provides the mapping of the vector between two time periods:

$$\mathbf{y}_m = (\mathbf{A}_{m-1}\mathbf{A}_{m-2}\cdots\mathbf{A}_0)\mathbf{y}_0 \ \Leftrightarrow\ \begin{pmatrix} x(t+2\pi) \\ \dot{x}(t+2\pi) \end{pmatrix} = \mathbf{\Phi}_m(2\pi)\begin{pmatrix} x(t) \\ \dot{x}(t) \end{pmatrix}\ , \tag{15}$$

where $\mathbf{\Phi}_m(2\pi)$ is the mth approximation of the so-called principal matrix of Floquet theory, the two eigenvalues of which determine the stability of the trivial solution in the same way as above, that is, their modulus has to be checked:

$$\det(\mu\,\mathbf{I} - \mathbf{\Phi}\,(2\pi)) = 0 \ \ \Rightarrow\ \ |\mu_{1,2}| \le 1 \ \Leftrightarrow\ \text{stability}. \tag{16}$$

Figure 5 shows the result of a calculation like this for the simplest case $m = 2$ when the calculation can still be carried out in closed form. This so-called Meissner[19] diagram already approximates the stable tongues of the stability chart in Fig.1 for the section $b = 0$ quite well.

The combination of the two approximations, namely, the combination of the time-periodic delay and the piece-wise constant periodic parametric excitation is quite straightforward and the finite dimensional approximation of the infinite dimensional principal operator of the Floquet theory can be given for any approximation number m. Consequently, the combination of examples (4) and (11) with increasing m converges to the stability regions of the delayed Mathieu equation

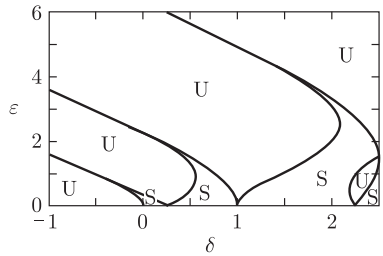

Fig. 5. Stable regions (S) of approximated harmonic parametric excitation equation (12) for $m = 2$.

in Fig.1. The method can be generalized to any linear time-periodic functional differential equation of the form (1) as proved by Insperger, Stepan, and Turi[20].

As an example, the stability chart of the damped delayed Mathieu equation

$$\ddot{x}(t) + \kappa \dot{x}(t) + (\delta + \varepsilon \cos t\,)x(t) = bx(t - 2\pi) \tag{17}$$

is presented in Fig.6 for $\varepsilon = 1$ and different values of the damping parameter κ.

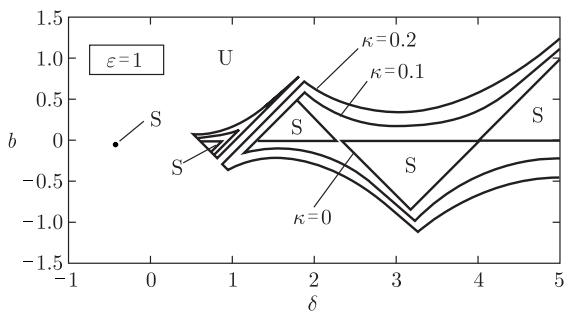

Fig. 6. Stable regions (S) of damped delayed Mathieu equation (17) by semi-discretization.

4. Engineering Applications

In the subsequent subsections, three engineering applications are presented where the mechanical models lead to the parametric excitation of delayed oscillatory systems and the stability analyses of the trivial solutions provide relevant information for the design and development of these structures.

4.1. *Modeling and Stability of Milling Operations*

Machine tools often have a characteristic lowest vibration mode. If this mode is approximated by a single degree-of-freedom oscillator of mass m, stiffness k, and (small) damping b, a parametrically excited delayed oscillator model can be derived

to describe the most critical vibrations of machine tools called chatter or regenerative vibrations.

The cutting force F_j acting on the jth cutting edge of the finger-like milling tool depends on the actual chip thickness $h(t)$ at the time instant t, and its variation can be approximated as a linear function of the chip thickness variation, which is proportional to the difference of two cutting edge positions: one is the past position of the preceding cutting edge at the time instant when it passed the same angular position, the other is the present position of the cutting edge. The resultant cutting force is the sum of the cutting force vectors acting at those cutting edges that are in contact with the workpiece. This leads to the mathematical model

$$m\ddot{x}(t) + b\dot{x}(t) + kx(t) = k_1(t)\left(x(t-\tau) - x(t)\right), \quad k_1(t+\tau) = k_1(t). \tag{18}$$

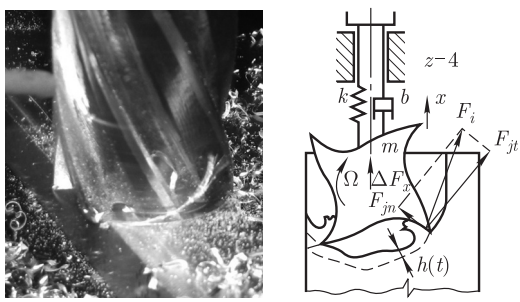

Fig. 7. Single degree-of-freedom mechanical model of milling.

The so-called cutting coefficient $k_1(t)$ is time-periodic with the time delay due to the periodic entering and leaving of the cutting edges into and from the material of the workpiece with the angular velocity Ω, that is, the period and the delay are both $\tau = 2\pi/\Omega$ (see details in Insperger, Stepan, Bayly, and Mann[21]).

The governing equation (17) is a generalized damped and delayed Mathieu equation with time-periodic parameters both in the stiffness and the gain parameter. The corresponding stability chart in Fig.8 is constructed by means of the semi-discretization method.

As predicted by the analytical stability chart of the delayed Mathieu equation, both Neimark-Sacker (that is, secondary Hopf) and flip (that is, period dobling) bifurcations occur at the stability limits. Figure 8 also shows the corresponding vibration frequencies at the stability limits and a typical time-variation of the cutting coefficient. All the parameters are dimensionless in the diagram, tilde refers to time-average value, $N = 4$ is the number of cutting edges, $f_n = \omega_n/(2\pi) = \sqrt{k/m}/(2\pi)$ is the natural frequency of the machine tool structure.

The stability charts, like the one in Fig.8, help engineers to design optimal cutting parameters where the material removal rate (MRR) is the largest, that is, the average cutting coefficient is maximized within the stability limit since it is

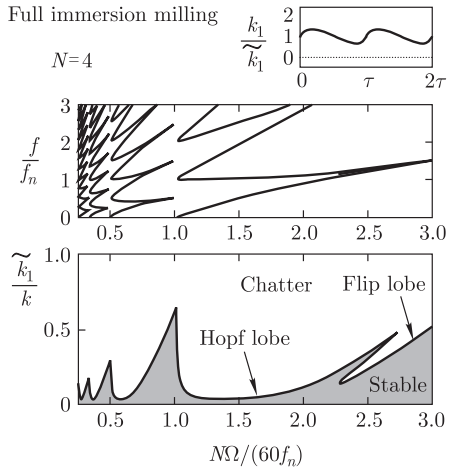

Fig. 8. Typical stability chart of full immersion milling operation and frequencies of self-excited vibrations at the stability limits also called lobes.

linearly proportional to the average chip width.

4.2. *Cutting with Varying Spindle Speed*

When turning processes are modeled as shown in Fig.9, the cutting coefficient is constant since there is always one cutting edge in contact with the workpiece. This means that there is no time-periodic stiffness or gain parameter in the governing equation, consequently, no flip bifurcations appear in the stability charts, only Hopf bifurcation occurs with a single frequency in it.

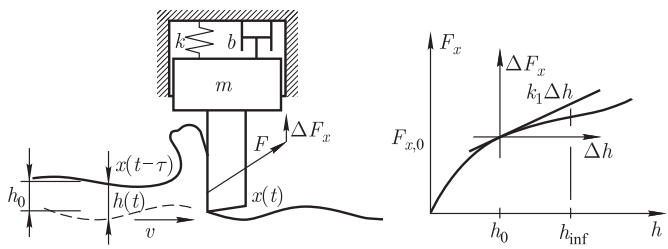

Fig. 9. Mechanical model of turning processes and the definition of the cutting coefficient k_1.

Still, the equation of motion includes time delay that is inversely proportional to the cutting speed v in the same way as explained above for milling. Parametric excitation can also be introduced by means of the periodic variation of the cutting speed, which results in a time-periodic time delay in the equation of motion:

$$m\ddot{x}(t) + b\dot{x}(t) + kx(t) = k_1 \left(x(t - \tau(t)) - x(t)\right), \quad \tau = \tau_0 + \tau_1 \cos(\omega_m t). \tag{19}$$

Now, the time period $2\pi/\omega_m$ of the time delay is, of course, different from the time

delay itself, but it can also be independent of the average value τ_0 of the delay. The stability chart of (19) is presented in Fig.10.

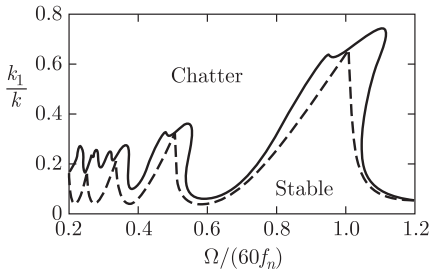

Fig. 10. Stability chart of (19) for spindle speed variation (continuous line) and for constant cutting speed (dashed line).

The stability chart of Fig.10 is presented with continuous lines for $T_m/\tau_0 = 2\pi/(\omega_m\tau_0) = 2$ and $\tau_1/\tau_0 = 0.1$ in case of spindle speed variation, while the stability boundaries are also presented with dashed lines for constant spindle speed when $\tau_1/\tau_0 = 0$. The calculations were carried out by the semi-discretization method in Insperger and Stepan[22]. The improvement in the stability of the turning process may be relevant for low cutting speeds when large periodic perturbation is introduced at the spindle speed. Similar results were obtained by Faassen, van de Wouw, Nijmeijer, and Oosterling[23].

4.3. *Act-and-wait Control of Force Controlled Robots*

Force control of robots often becomes unstable due to the presence of digital effects and time delays in the control loop. Figure 11 presents a single degree-of-freedom model of force control where the uncontrolled system has an undamped angular natural frequency ω_n and damping ratio ζ. The sampling time in the digital control is denoted by Δt, and we consider a time delay in the loop which is characterized by the integer r referring to a delay $r\Delta t$ in the loop.

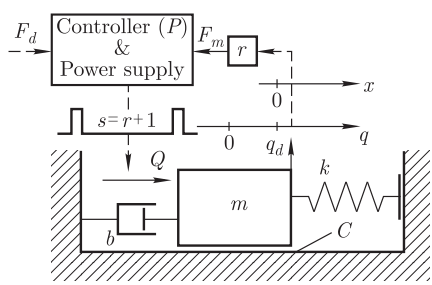

Fig. 11. Mechanical model of force control with act-and-wait feedback.

The desired contact force is $F_d = kq_d$ where q denotes the position of the robotic arm that touches the environment via the spring of stiffness k, while the measured or sensed force is $F_m = kq$. The traditional proportional control applies the control force

$$Q(t) = F_d - P(F_m(t_{j-r}) - F_d), \quad t \in [t_j, t_{j+1}), \quad t_j = j\Delta t, \quad j = 0, 1, 2, \ldots, \tag{20}$$

where P is a dimensionless proportional gain and t_j is the jth sampling instant of the digital control. In the presence of a Coulomb friction force C, this results in a static force error $F_e = C/(1 + P)$ around the desired force F_d, which can be decreased by the increase of the gain P. However, there is a maximum value for the gain P above which the desired position of the system becomes unstable and self-excited vibrations appear. The larger the sampling time Δt and/or the time delay $r\Delta t$ are, the smaller this maximal gain is, and consequently, the larger the static error of the system is.

The application of a time-periodic gain in the control loop gives the possibility to increase the maximum values of the gain and so to decrease the static force error. As it is explained in the introduction of the so-called act-and-wait control strategy by Stepan and Insperger[24], a quasi optimal time-periodicity is achieved when the proportional control is switched on and off, as represented in Fig.11 by the $s\Delta t$ periodicity of the control force in Fig.11:

$$Q_{a\&w}(t) = \begin{cases} F_d - P(F_m(t_{j-r}) - F_d), & \text{if} \quad t \in [t_{hs}, t_{hs+1}), \quad h \in \mathbb{Z}, \\ F_d, & \text{otherwise} \end{cases} \tag{21}$$

with subscript $a\&w$ referring to act-and-wait.

If the small perturbation x is introduced by $q(t) = q_d + x(t)$ around the desired position of the system, the equation of motion assumes the form

$$\ddot{x}(t) + 2\zeta\omega_n\dot{x}(t) + \omega_n^2 x(t) = -g_j\omega_n^2 P x(t_{j-r}) \,, \qquad t \in [t_j, t_{j+1}) \,, \tag{22}$$

where a switching function g_j is introduced by

$$g_j = \begin{cases} 1, & \text{if} \quad j = hs, \quad h \in \mathbb{Z}, \\ 0, & \text{otherwise} \end{cases} \tag{23}$$

corresponding to the act-and-wait control force (21). The actual interpretation of (22) is that it is a time periodic DDE with a piece-wise constant periodic parametric excitation at the gain and a piece-wise linear parametric excitation at the time delay. The stability of the trivial solution can be analyzed directly in the discrete state space representation with $\mathbf{y} = \mathrm{col}(x\ \dot{x}) \in \mathbb{R}^2$:

$$\begin{aligned} &\mathbf{y}(j+1) = \mathbf{Q}\mathbf{y}(j) + \mathbf{R}\mathbf{w}(j-r), \\ &\mathbf{w}(j) = g_j\mathbf{H}\mathbf{x}(j), \end{aligned} \tag{24}$$

where the matrices are defined as

$$\mathbf{Q} = \exp(\mathbf{A}\Delta t) \,, \quad \mathbf{R} = (\exp(\mathbf{A}\Delta t) - \mathbf{I})\mathbf{A}^{-1}\mathbf{B} \,, \quad \mathbf{H} = [\,-\omega_n^2 P, \;\; 0\,] \,, \tag{25}$$

and the matrices $\mathbf{A}$ and $\mathbf{B}$ are given by the DDE (22) in the form

$$\mathbf{A} = \begin{bmatrix} 0 & 1 \\ -\omega_n^2 & -2\zeta\omega_n \end{bmatrix}, \quad \mathbf{B} = \begin{bmatrix} 0 \\ 1 \end{bmatrix}. \tag{26a}$$

In the same way as the semi-discretization method was introduced, a discrete map

$$\underbrace{\begin{bmatrix} \mathbf{y}(j+1) \\ \mathbf{w}(j) \\ \mathbf{w}(j-1) \\ \vdots \\ \mathbf{w}(j-r+1) \end{bmatrix}}_{\mathbf{z}_{j+1}} = \underbrace{\begin{bmatrix} \mathbf{Q} & \mathbf{0} & \cdots & \mathbf{0} & \mathbf{R} \\ g_j\mathbf{H} & \mathbf{0} & \cdots & \mathbf{0} & \mathbf{0} \\ \mathbf{0} & \mathbf{I} & \cdots & \mathbf{0} & \mathbf{0} \\ \vdots & \vdots & & \vdots & \vdots \\ \mathbf{0} & \mathbf{0} & \cdots & \mathbf{I} & \mathbf{0} \end{bmatrix}}_{\mathbf{G}_j} \underbrace{\begin{bmatrix} \mathbf{y}(j) \\ \mathbf{w}(j-1) \\ \mathbf{w}(j-2) \\ \vdots \\ \mathbf{w}(j-r) \end{bmatrix}}_{\mathbf{z}_j} \tag{26b}$$

can be constructed where the coefficient matrix varies with periodicity s in accordance with the definition of the switching function g_j in (23). If the discrete maps are concatenated, the linear discrete map has the form

$$\mathbf{z}_s = \mathbf{G}_{s-1}\cdots\mathbf{G}_1\mathbf{G}_0\mathbf{z}_0 \;\Rightarrow\; \mathbf{z}_s = \mathbf{G}_1^{s-1}\mathbf{G}_0\mathbf{z}_0 \;\Rightarrow\; \mathbf{z}_s = \mathbf{\Phi}_{r,s}\mathbf{z}_0\,, \tag{27}$$

where the matrix $\mathbf{\Phi}_{r,s}$ is the actual form of the principal operator of the periodic DDE (23) with periodicity s and delay r.

It is shown by Insperger, Wahi, Colombo, Stepan, di Bernardo, Hogan[25] that the largest stable parameter domains can be achieved when the period s is just larger than the delay r, so when $s = r+1$, as it is also represented in Fig.11. The stability chart in Fig.12 is constructed for the modal parameters of a Hirata robot used in laboratory experiments. The stability limits and the frequencies of the emerging self-excited vibrations are presented by grey lines for constant proportional gains and by black lines for periodically varying gains with $r = 1,\ s = 2$. Apart of the Hopf bifurcation, flip bifurcations can occur in case of the act-and-wait control, while the maximal gains within the stability limits are doubled in this case, which means that the static force error is reduced by a factor of 2.

These theoretical predictions were also confirmed experimentally in Insperger, Kovacs, Galambos, and Stepan[26] where the force control of a Hirata robot was established: the robotic arm pushed a helical spring with a prescribed (or desired) contact force against a fixed wall. After the accurate identification of the modal parameters, the above calculations were repeated and the theoretical and the experimental results are compared in Fig.12.

5. Conclusions

Parametric excitation may cause vibration phenomena that are often difficult to handle in certain engineering tasks. Time delays may also cause unexpected self-excited vibrations even for very small delays. When parametric excitation appears in combination with time delays, the emerging vibrations are often intricate, quasi

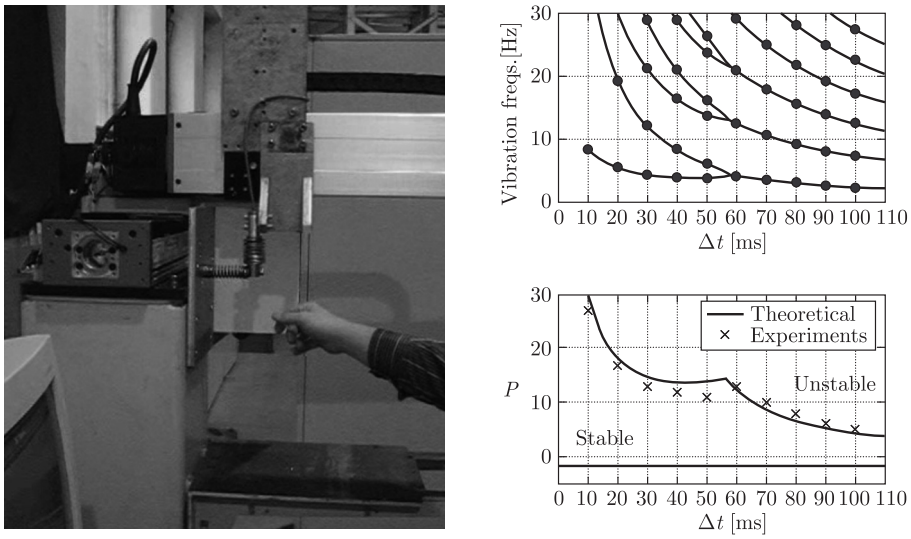

Fig. 12. Force controlled Hirata robot in laboratory experiments and experimental stability chart with measured and theoretically predicted vibration frequencies of self-excited vibrations originated in Hopf and period doubling bifurcations.

periodic or even chaotic, and it is difficult to find where and how to tune the system parameters to eliminate them.

The mathematical models of parametrically excited delayed oscillators are time-periodic delay-differential equations. Their linearization and stability analysis requires the application of an infinite dimensional Floquet theory. The application of the theory for engineering problems is difficult due to the lack of analytically proven reference examples and efficient numerical methods.

The delayed Mathieu equation paradigm is an essential example for a delayed oscillator subjected to harmonic parametric excitation at the stiffness. The stability chart was constructed analytically, which means that it can serve as a reference example for testing numerical methods. Among the numerical methods, the basic idea of the semi-discretization method was described (see Insperger and Stepan[27]) as a time-periodic perturbation of the time delay.

The efficiency of the introduced method was presented in case of three relevant engineering problems. In case of cutting operations, the time delay occurs due to the contact of the tool and the workpiece. Milling operations involve time periodic parametric excitation with time period equal to the time delay. In case of turning, this kind of parametric excitation cannot occur, but the time-periodic spindle speed variation results parametric excitation at the delay. This can be used to improve the stability properties of turning processes. The third example discussed in this study is the act-and-wait force control, where time periodic gains are used to improve the stability properties and to decrease the static force error of force controlled robots.

The exploration of the stability properties of time-periodic delayed oscillators partly helps understanding the peculiar vibration properties of these systems, partly it helps to explore new parameter domains where those delayed systems can be stabilized with parametric excitation, which would be unstable otherwise.

Acknowledgments. The research work was supported by the Hungarian National Science Foundation under grant no. OTKA K101714 and it is also connected to the scientific program of the "Development of quality-oriented and harmonized R+D+I strategy and functional model at BME" project. This project is supported by the New Szechenyi Plan, Project ID: TAMOP-4.2.1/B-09/1/KMR-2010-0002.

References

1. A. D. Myshkis, *Lineare Differentialgleichungen mit Nacheilendem Argument* (Deutscher Verlag der Wissenschaften, Berlin, 1955).
2. A. Halanay, Stability theory of linear periodic systems with delay (in Russian), *Rev Roum Math Pure A*, **6**, 633–653 (1961).
3. J. K. Hale, *Theory of Functional Differential Equations* (Springer-Verlag, New York, 1977).
4. J. K. Hale and S. M. V. Lunel, *Introduction to Functional Differential Equations* (Springer-Verlag, New York, 1993).
5. V. Volterra, Sur la theorie mathematique des phenomenes hereditaires, *J. Math. Pure Appl.*, **7**, 149–192 (1928).
6. E. Mathieu, Memoire sur le mouvement vibratoire d'une membrane de forme elliptique, *J. Math. Pure Appl.*, **13**, 137–203 (1868).
7. S. J. Bhatt and C. S. Hsu, Stability criteria for second-order dynamical systems with time lag. *J. Appl. Mech-T ASME*, **33**, 113–118 (1966).
8. F. van der Pol and M. J. O. Strutt, On the stability of the solutions of Mathieu's equation, *Philosophical Magazine and Journal of Science*, **5**, 18–38 (1928).
9. E. L. Ince, *Ordinary Differential Equations* (Longmans, Green and Co., London, 1926).
10. G. Stepan, *Retarded Dynamical Systems* (Longman, Harlow, 1989).
11. H. Hu and Z. Wang, *Dynamics of Controlled Mechanical Systems with Delayed Feedback* (Springer, Berlin, 2002).
12. W. Michiels and S. I. Niculescu, *Stability and Stabilization of Time-delay Systems*: *an Eigenvalue-based Approach* (SIAM Publications, Philadelphia, 2007).
13. T. Insperger and G. Stepan, Stability chart for the delayed Mathieu equation, *Proc. R. Soc. Lond A–Math Phy.*, **458**, 1989–1998 (2002).
14. T. Insperger and G. Stepan, Semi-discretization method for delayed systems. *Int. J. Numer. Meth. Eng.*, **55**, 503–518 (2002).
15. J. Sheng, O. Elbeyli, and J. Q. Sun, Stability and optimal feedback controls for time-delayed linear periodic systems, *AIAA J.*, **42**, 908–911 (2004).
16. P. V. Bayly, J. E. Halley, B. P. Mann, and M. A. Davies, Stability of interrupted cutting by temporal finite element analysis, *J. Manuf. Sci. E–T ASME*, **125**, 220–225 (2003).
17. E. A. Butcher, H. Ma, E. Bueler, V. Averina, and Z. Szabo, Stability of linear time-periodic delay-differential equations via Chebyshev polynomials, *Int. J. Numer. Meth. Eng.*, **59**, 895–922 (2004).

18. D. Breda, S. Maset, and R. Vermiglio, Pseudospectral differencing methods for characteristic roots of delay differential equations, *SIAM J. Sci. Comput.*, **27**, 482–495 (2005).
19. R. Zurmuhl, *Numerische Behandlung von Schwingungsaufgaben mittels Übertragungsmatrizen* (Dusseldorf, VDI, 1959).
20. T. Insperger, G. Stepan, and J. Turi, On the higher-order semi-discretizations for periodic delayed systems, *J. Sound Vib.*, **313**, 334–341 (2008).
21. T. Insperger, G. Stepan, P. V. Bayly, and B. P. Mann, Multiple chatter frequencies in milling processes, *Journal of Sound and Vibration*, **262**, 333–345 (2003).
22. T. Insperger and G. Stepan, Stability analysis of turning with periodic spindle speed modulation via semi-discretization, *J. Vib. Control*, **10**, 1835–1855 (2004).
23. R. P. H. Faassen, N. van de Wouw, H. Nijmeijer, and J. A. J. Oosterling, An improved tool path model including periodic delay for chatter prediction in milling, *J. Comput. Nonlin. Dyn–T ASME*, **2**, 167–179 (2007).
24. G. Stepan and T. Insperger, Stability of time-periodic and delayed systems — a route to act-and-wait control, *IFAC Annual Reviews in Control*, **30**, 159–168 (2006).
25. T. Insperger, P. Wahi, A. Colombo, G. Stepan, M. di Bernardo, and J. S. Hogan, Full characterization of act-and-wait control for first order unstable lag processes, *Journal of Vibration and Control*, **16**, 1209–1233 (2010).
26. T. Insperger, L. L. Kovacs, P. Galambos, and G. Stepan, Increasing the accuracy of digital force control process using the act-and-wait concept, *IEEE-ASME T Mech.*, **15**, 291–298 (2010).
27. T. Insperger and G. Stepan, *Semi-discretization for Time-delay Systems* (Springer, New York, 2011).